Flow Shear Stabilization of Ion Temperature Gradient Modes in an Internal Transport Barrier

J. Q. Dong
Southwestern Institute of Physics, P. O. Box 432 Chengdu, China
e-mail contact of main author: jqdong@chungtze.ps.uci.edu

Abstract Ion temperature gradient (ITG) driven instability is studied with gyrokinetic theory in an internal transport barrier (ITB) of tokamak plasmas. The stabilization effects of a parallel ve1ocity shear on the modes are investigated. It is found that the mode structures and stability properties, as well as the effects of a velocity shear, in an ITB are significantly different from that in off-ITB regions.

1. Introduction

One of the most significant achievements in tokamak experiments in recent years is the discovery of internal transport barrier (ITB).[1-3] An ITB is characterized by steep temperature and density gradients near the $q_{\rm min}$-surface where the magnetic shear approaches zero. A common understanding for the formation mechanism of an ITB is stabilization of a variety of micro-instabilities by a negative central magnetic shear and by a perpendicular velocity shear.[4] However, experimental data clearly show that ITBs are not limited to radial regions with reversed shear, but extend deep into the region of reduced positive shear. In other words, the location of an ITB coincides with or is close to the $q_{\rm min}$-position. Therefore, the best confinement is measured precisely in the regions of very weak magnetic shear (VWS).[1,5]

In addition, toroidal (parallel) ion velocities with nonmonotonous profiles are often observed in ITBs experimentally. The maximum/minimum of the velocity is mostly located close to the edge of the ITB.[1,3] Nevertheless, effects of velocity shear on instabilities in plasmas of VWS are rarely studied.

As a part of the effort to understand the mechanism for the formation of an ITB, and for the sake of the completeness of ITG instability theory, in present work, the ITG modes are reconsidered with the effects of a parallel velocity shear included. The gyro-kinetic theory, with finite Larmor radius effects retained, is employed in a sheared slab of VWS.

The physics model and dispersion equation are given in Section 2. The numerical results are presented in Section 3, and Section 4 is devoted to conclusions and discussion.

2. Physics Models and Dispersion Equation

In order to describe ion dynamics near a $q_{\rm min}$-surface adequately, the second derivative of the safety factor q with respect to the radial variab1e r has to be taken into account. A sheared slab model is, then, extended to include the variation of magnetic shear,

$$\mathbf{B} = B_0[\hat{\mathbf{z}} + (\frac{x}{L_s} + \frac{x^2}{L_{s2}})\hat{\mathbf{y}}], \tag{1}$$

where

$$\frac{1}{L_s} = -\frac{r_0 q_0'}{R q_0^2} = -\frac{s}{R q_0}, \quad \frac{1}{L_{s2}} = -\frac{r_0}{2R q_0^2}\frac{d^2 q}{dr^2} + \frac{r_0}{R q_0^3}\left(\frac{dq}{dr}\right)^2 = -\frac{\hat{s}_d}{R q_0}, \tag{2}$$

$x = r - r_0$. As is usually understood, equilibrium quantities, such as safety factor q, magnetic shear s and scale lengths L_j etc., as well as the derivatives all have the values at the surface of $r = r_0$. The most important change introduced by the gradient of magnetic shear takes place in the wave-particle interaction argument,

$$\zeta_i = \frac{\omega}{|k_{\|}| v_{ti}} = \frac{\sqrt{\tau}}{2}\frac{\hat{\omega}}{|x(\hat{s} + s_2 x)|}, \tag{3}$$

where

$$\hat{\omega} = \frac{\omega}{\omega_{*e}}, \quad \hat{s} = \frac{L_n}{L_s}, \quad s_2 = \frac{L_n \rho_i}{L_{s2}}, \quad \tau = T_e/T_i, \quad \omega_{*e} = \frac{c k_y T_e}{e B L_n}, \tag{4}$$

The parameter s_2 introduces a second resonant surface at $x_1 = -\hat{s}/s_2$, besides the one at $x = 0$ and, therefore, new features of the ITG instability.

Gyrokinetic theory is employed for ions. Electrons are adiabatic. Electrostatic perturbations are considered and assumed in the form,

$$\tilde{f}(x, y, t) \sim \tilde{f}(x) e^{-i\omega t + i k_y y}$$

The eigenmode equation is then obtained from the quasi-neutrality condition as [6]

$$[1 + \tau - (\tau + \frac{1}{\hat{\omega}})\Gamma_0(k_\perp) + \frac{\eta_i k_\perp^2}{2\hat{\omega}}(\Gamma_0(k_\perp) - \Gamma_1(k_\perp))]\hat{\phi}(k) + \int_{-\infty}^{+\infty} \frac{dk'}{\sqrt{2\pi}} K(k, k')\hat{\phi}(k') = 0, \tag{5}$$

where

$$K(k, k') = \frac{1}{\sqrt{2\pi}}\int_{-\infty}^{+\infty} dx e^{i(k'-k)x} \times \{\left[(\tau + \frac{1}{\hat{\omega}})\Gamma_0(k_\perp, k_\perp') + \frac{\eta_i}{\hat{\omega}}(b\Gamma_1(k_\perp, k_\perp') - b_1\Gamma_0(k_\perp, k_\perp')\right] \times$$
$$(1 + \zeta_i Z(\zeta_i)) + \frac{\eta_i}{\hat{\omega}}\left[\zeta_i^2 + \left(\zeta_i^2 - \frac{1}{2}\right)\zeta_i Z(\zeta_i)\right] \Gamma_0(k_\perp, k_\perp') - 2\hat{v}_0' \frac{\omega_{*e}}{k_{\|} v_{ti}}(1 + \zeta_i Z(\zeta_i))\Gamma_0(k_\perp, k_\perp')\}, \tag{6}$$

$Z(\zeta_i)$ is the plasma dispersion function, and

$$b = \frac{k_\perp k_\perp'}{2}, \quad b_1 = \frac{k_\perp^2 + k_\perp'^2}{4}, \quad k_\perp^2 = k_y^2 + k^2, \quad k_\perp'^2 = k'^2 + k_y^2, \quad \eta_i = L_n/L_{Ti}, \tag{7}$$

$\hat{v}_0' = (L_n/c_s)(dv_0/dx)$ is the normalized parallel velocity shear, L_n L_{Ti} are the density and temperature gradient scale lengths, respectively; k, k' and k_y are normalized to $\rho_i^{-1} = eB/c\sqrt{2T_i m_i}$, x is normalized to ρ_i.

$$\Gamma_j(k_\perp, k_\perp') = I_j\left(\frac{k_\perp k_\perp'}{2}\right)\exp\left[-\frac{(k_\perp^2 + k'^2_\perp)}{4}\right], \quad \Gamma_j(k_\perp) = I_j\left(\frac{k_\perp^2}{2}\right)\exp\left[-\frac{k_\perp^2}{2}\right], \tag{8}$$

where I_j is the modified Bessel function of order $j = (0, 1)$.

3. Numerical Results

The integral eigenmode equation, Eq. (5), is solved numerically with schemes well documented.[7] The parameters employed are $\eta_i = 4,\ \tau = 1, k_y = 0.35$, unless otherwise stated. The signs of $\widehat{s}$, s_2 and $\widehat{s}/s_2$ do not introduce essential effects into the subject. Therefore, $\widehat{s} > 0$ ($s < 0$) and $s_2 < 0$ ($\widehat{s}_d > 0$) are considered only.

The normalized mode growth rate (a) and real frequency (b) are shown in Fig. 1 as functions of magnetic shear $\widehat{s}$ for $s_2 = -0.01$. For a given set of plasma parameters, four distinct unstable branches emerge in the regime of VWS ($\widehat{s} \lesssim 0.1$). The modes are titled as D (the lines without symbol), D' (the lines with closed circles), G (the lines with triangles) and G' (the lines with open circles) branches, respectively, in this work.

The corresponding eigenfunctions $\tilde{\phi}(x)$ of the four branches are shown in Fig. 2 for $\widehat{s} = 0.01$. The lines with open and closed circles are the real and imaginary parts, respectively. As is pointed out in the last Section, there are two resonant surfaces at $x = 0$ and $x = x_1$ when the gradient of the magnetic shear, s_2, is taken into account. In addition, there are two unstable modes, with even and odd parities, respectively, centered at each resonant surface. The modes centered at $x = 0$ are strongly coupled with that centered at $x = x_1$ when the magnetic shear is weak enough such that $x_1 \lesssim$ wavelength of the modes. The four branches result from different couplings between the four modes. The D (Fig.2(a)) and G (Fig.2(b)) branches are from the coupling of the two even and two odd modes centered at $x = 0$ and $x = x_1$, respectively. Meanwhile, the D' (Fig.2(c)) and G' (Fig.2(d)) branches stem from the coupling between one even and one odd mode, respectively. As a result, the D and G branches are even, while the D' and G' branches are odd.

In Fig. 1, the branches D and D' merge to one branch at $\widehat{s} \gtrsim 0.15$ where $|s_2/\widehat{s}| \ll 1$ and the mode located at $x = x_1 = -\hat{s}/s_2$ is far away and decoupled from the mode at $x = 0$. The merged branch is the lowest even parity mode and, therefore, the continuation of the branch D. On the other hand, the branch D' is introduced by s_2 and, therefore, disappears for $|s_2/\widehat{s}| \ll 1$. The same is true for the branches G and G' except that the merged branch has odd parity.

The effects of parallel velocity shear $\widehat{v}_0'$ on the modes are presented in Fig. 3. The lines without symbols and with closed circles are for D and G branches, respectively, while the lines with open circles and triangles are for D' and G', respectively.

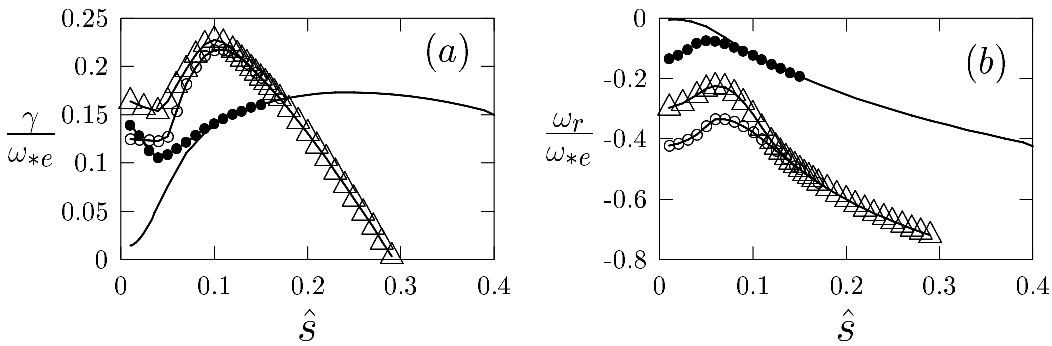

FIG.1. Normalized growth rate (a) and real frequency (b) versus magnetic shear.

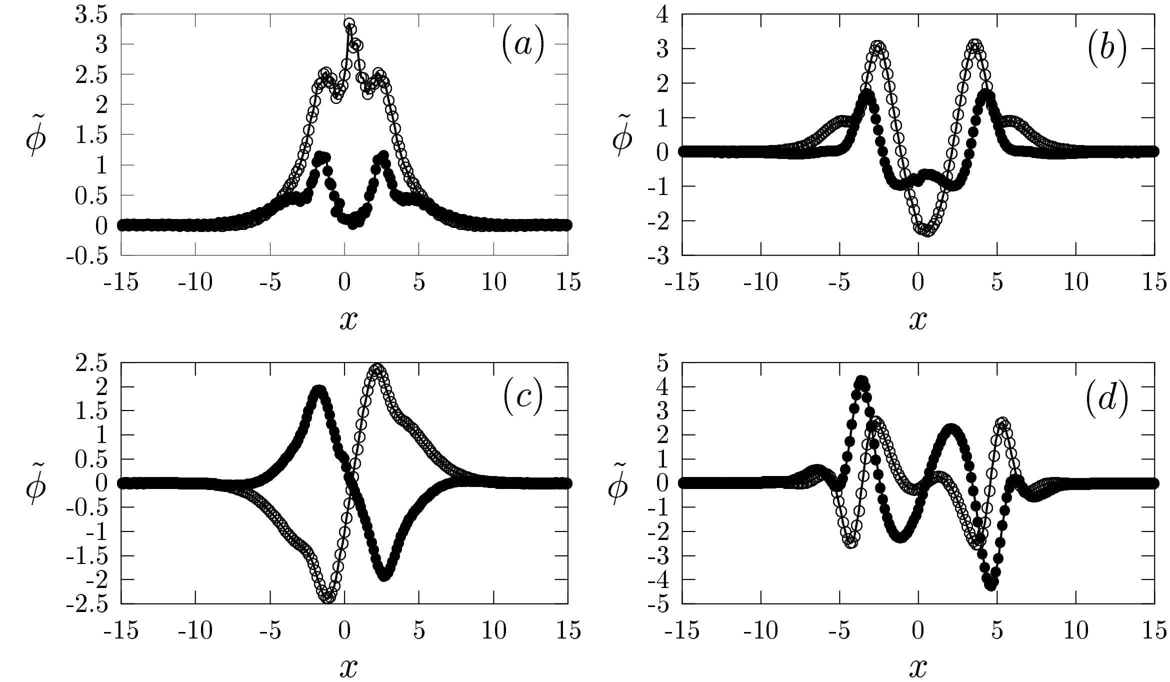

FIG. 2. Eigenfunctions of D (a), D' (b),
G (c) and G' (d) branches for $\hat{s} = 0.01$ and $s_2 = -0.01$.

It is evident that the growth rate of the modes is sensitive to the sign of $\widehat{v}_0'$. A negative $\widehat{v}_0'$ is destabi1izing while a positive $\widehat{v}_0'$ is stabi1izing. The physics understanding is that a $\widehat{v}_0'$ introduces a position shift, $\Delta \sim \widehat{v}_0'/\widehat{s}$, of the mode originally centered at $x = 0$, that may enhance or weaken the coup1ing between the modes originally centered at $x = 0$ and $x = x_1$, depending on the sign of $\widehat{v}_0'$. This observation is further proven by the fact that the effects of $\widehat{v}_0'$ are reversed when $\widehat{s}$ and s_2 have same sign. As a comparison, the results of the D (the lines with crosses) and G (the lines with diamonds) branches for $\widehat{s} = .25$ are shown to be independent of the sign of $\widehat{v}_0'$ in Fig. 3.

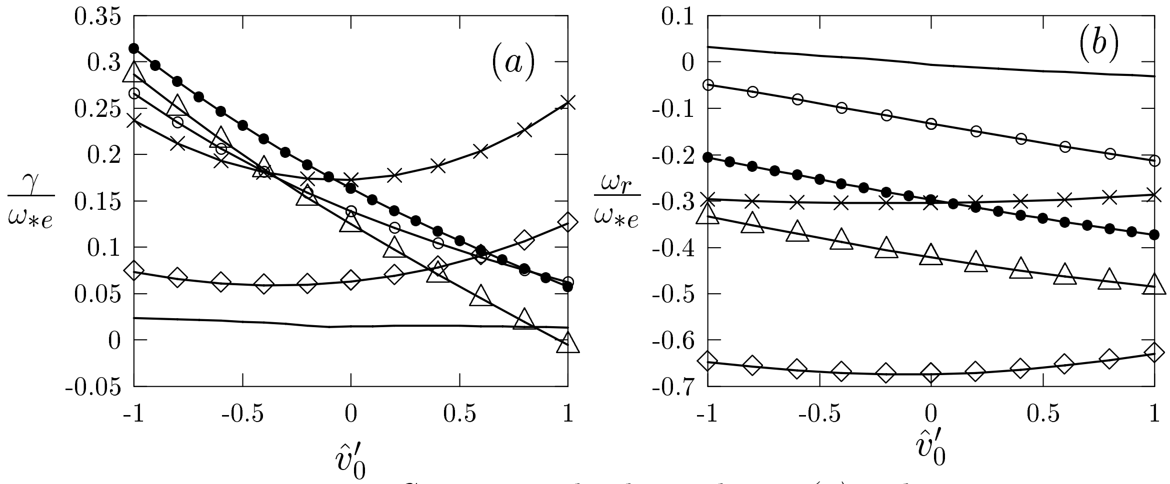

FIG. 3. Normalized growth rate (a) and
real frequency (b) of the modes versus $\widehat{v}_0'$ for $s_2 = -0.01$ and $\widehat{s} = 0.01$.

4. Conclusions and Discussion

The ion temperature gradient modes are studied in an ITB with a VWS. Effects of the gradients of magnetic shear are taken into account. Four distinct branches are found simultaneously unstable. The effects of a parallel velocity shear v_0' on the modes in an ITB with VWS are found to be significantly different from those in moderate or strong shear regimes. The growth rates and real frequencies of the modes are sensitive to the sign of $\widehat{v}_0'$ for the former while they are independent of the sign for the latter. For the former, a negative $\widehat{v}_0'$ is suppressing while a positive $\widehat{v}_0'$ is driving when the signs of magnetic shear $\widehat{s}$ and gradient of the magnetic shear s_2 are opposite to each other. The $\widehat{v}_0'$ effects are reversed when the signs of $\widehat{s}$ and s_2 are same.

The results here are in qualitative agreement with the observations on JT-60U which show that the ITB is located in the region of $\widehat{v}_0' > 0$ and one of its edges coincides with the position of $\widehat{v}_0' = 0$.[1] For quantitative comparison with experiments, non-linear simulations in a toroidal geometry are needed.

Acknowledgments

The last version of this work was completed during the author's visit at the National Institute for Fusion Science, Japan. He would like to thank the staff of NIFS for their hospitality. This work is supported by NSFC Grant No.19875014.

References

[1] KOIDE, Y., *et al.*, "Progress in confinement and stability with plasma shape and profile control for steady-state operation in Japan Atomic Energy Research Institute Tokamak-60 Upgrade", Phys. Plasmas **4** (1997) 1623.

[2] STRAIT, E. J., *et al.*, "Enhanced confinement and stability in DIII-D discharges with reversed magnetic shear", Phys. Rev. Lett. **75** (1995) 4421.

[3] LAO, L. L., *et al.*, "Rotation and magnetic shear stabilization of magnetohydrodynamic modes and turbulence in DIII-D high performence discharges", Phys. Plasmas **3** (1996) 1951.

[4] LEVINTON, F. M., *et al.*, "Improved confinement with reversed magnetic shear in TFTR", Phys. Rev. Lett. **75** (1995) 4417.

[5] FUJITA, T., *et al.*, "Internal transport barrier for electrons in JT-60U reversed shear discharges", Phys. Rev. Lett. **78** (1997) 2377.

[6] DONG, J. Q., *et al.*, "Finite beta effects on ion temperature gradient driven modes", Phys. Fluids **30** (1987) 2694.

[7] DONG, Jiaqi, *et al.*, "Study of kinetic shear Alfvén modes driven by ion temperature gradient in tokamak plasmas", Nucl. Fusion **39** (1999) 1041.